Comparisons between Monte Carlo simulations and a simple crossing-symmetric approach to the Hubbard model at low density

Anne-Marie Daré, Liang Chen, and A.-M. S. Tremblay
Département de Physique and Centre de Recherche en Physique du Solide, Université de Sherbrooke, Sherbrooke, Québec, Canada J1K 2R1
(Received 12 July 1993)

A simple crossing-symmetric approximation for the fully reducible vertex is compared with Monte Carlo simulations of the two-dimensional Hubbard model. Up to quarter-filling, in the intermediate coupling regime, accuracies better than 10% are obtained for several static correlation functions, including spin and charge, as well as the pairing channels most widely studied in the context of high-T_c superconductivity. The accuracy is generally better for the pairing channels. The results shed light on the applicability of the renormalized generalized-random-phase-approximation scheme, its relation to Fermi-liquid theory, and on the regime where nontrivial effects may appear in pairing channels. The approximation under study consists in assuming that for parallel spins the *fully reducible* particle-particle vertex vanishes, while for antiparallel spins it is equal to the T matrix. The fully reducible particle-hole vertex is then obtained from the latter vertex by using crossing symmetry. This simple approximation is not conserving but it preserves global symmetries. It suggests that Monte Carlo results for the two-dimensional Hubbard model in small systems at low density and intermediate coupling can be interpreted using a weakly correlated Fermi-liquid picture.

I. INTRODUCTION

There are two broad classes of self-consistent approximations used in calculating correlation functions of many-body systems: conserving[1–3] and crossing symmetric.[4,5] Conserving approximations obtained from simple self-energy diagrams following the Baym-Kadanoff approach[1] are not crossing symmetric[6] and there is no known general scheme which guarantees that a crossing-symmetric *approximation* will also be conserving. It is known, however, that for the one-band Hubbard model, self-consistent crossing-symmetric approximations built on parquet equations give better agreement with Monte Carlo calculations than self-consistent conserving approximations.[7]

Given the complexity of the above calculations, it is still useful to have some simpler approximation schemes which (a) are easier to generalize to more complex models than the nearest-neighbor Hubbard model and (b) give more insight into the physics.

In this paper, we investigate a simple approximation scheme which is based on crossing symmetry and which is remarkably accurate in the low-density limit. More specifically, we assume that for parallel spins the *fully reducible* particle-particle vertex vanishes, while for antiparallel spins it is equal to the T matrix. The fully reducible particle-hole vertex is then obtained from the latter vertex by using crossing symmetry. This simple approximation is not conserving but it preserves global symmetries. We show that in the intermediate-coupling regime ($U \sim \frac{1}{2}$ bandwidth) most widely studied in Monte Carlo simulations, accurate results are obtained for spin, charge, and pairing correlation functions. Although results in the pairing channel are generally better than in the particle-hole channels, up to about quarter-filling all the usual static correlation functions obtained by Monte Carlo simulations in both the particle-hole and particle-particle channels are reproduced to better than 10%.

There has been some controversy concerning the existence of a Fermi liquid in two dimensions, even in the low-density limit.[8,9] We show in an appendix that in the low-density intermediate-coupling regime described above, the Monte Carlo simulations are consistent with a very weakly correlated Fermi-liquid picture. This Fermi-liquid point of view also sheds light on an approximation scheme which was proposed earlier:[10–12] In this approximation, magnetic correlation functions can be quite accurately computed even in the intermediate-coupling regime by using the standard generalized-random-phase-approximation (GRPA) scheme, with a renormalized value of the interaction U. It was proposed that the renormalization comes from short-range T-matrix effects, and hence may be estimated.

In Sec. II, we define our diagrammatic approach. Section III is devoted to detailed comparisons between our approach and Monte Carlo results for (a) particle-hole correlation functions (density and magnetic fluctuations) and (b) particle-particle correlation functions which appear in various pairing channels of interest in the context of high-temperature superconductivity. Ward identities for the Hubbard model, as well as the validity of the GRPA approximation with renormalized U and its relation to Fermi-liquid theory, are discussed in the appendices. It is also explained in the last two appendices why the agreement for dynamical correlation functions may not be so good. Note that in all our calculations we have no control over long-wavelength effects[13] since we are comparing with small-system simulations. Finite-size effects have been a problem in detecting non-Fermi-liquid effects in one-dimensional systems,[14] hence one should remain careful in interpreting the results.

0163-1829/94/49(6)/4106(13)/$06.00

II. CROSSING-SYMMETRIC APPROXIMATION FOR THE PARTICLE-PARTICLE AND PARTICLE-HOLE VERTICES

We consider the two-dimensional Hubbard model,

$$H=-t\sum_{\langle i,j\rangle,\sigma}(c_{i\sigma}^{\dagger}c_{j\sigma}+c_{j\sigma}^{\dagger}c_{i\sigma})+U\sum_{i}n_{i\uparrow}n_{i\downarrow}-\mu\sum_{i,\sigma}n_{i\sigma}\ , \tag{1}$$

where the first sum is over nearest-neighbor pairs. It is known since the work of Galitskii,[15] Brueckner *et al.*,[16] and Kanamori[17] that for short-range potentials, the two-body potential (U above) should be replaced by the T matrix in computing low-energy properties. We go one step further for the Hubbard model by approximating the fully reducible vertex by the T matrix and using this single vertex in *all* channels. In this approximation, only electrons of opposite spin scatter and the fully reducible vertex is, in fact, irreducible in the particle-hole channel. The fully reducible vertex then is approximated by the particle-particle vertex illustrated diagrammatically in Fig. 1. Analytically, we write,

$$\Gamma(1,2;3,4,)=T(1+2 \text{ or } 3+4)\delta_{1,\bar{2}}(\delta_{1,4}\delta_{2,3}-\delta_{1,3}\delta_{2,4})\ , \tag{2}$$

where $1=(1,1)$ with $1=(\mathbf{k}_1,\omega_1)$ standing for both the Matsubara frequency and two-dimensional wave vector, and 1 standing for the spin index ($\bar{1}$ is the opposite spin). In the above expression then, all δ functions are on spin indices. In this approximation, incoming particles scatter only if they have opposite spins. As usual, the expression for the T matrix is

$$T(1+2 \text{ or } 3+4)=\frac{U}{1+U\chi_{pp}(\mathbf{k}_1+\mathbf{k}_2,\omega_1+\omega_2)}\delta(1+2-3-4) \tag{3}$$

with

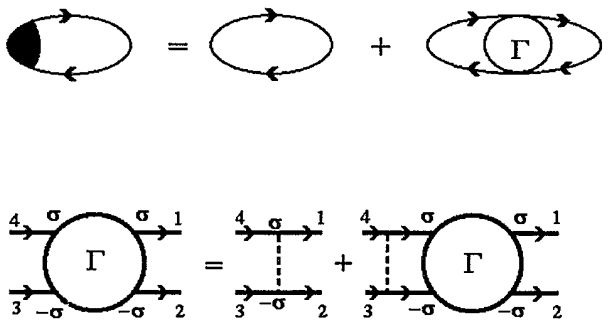

FIG. 1. Definition of the fully reducible vertex Γ and its approximation in terms of the T matrix. The vertex vanishes when the spins of all particles are identical. There is an extra minus sign when two particles are exchanged in either the initial or the final state.

$$\chi_{pp}(1)=\frac{1}{\beta N}\sum_{1'}G(-1')G(1+1')\ . \tag{4}$$

(The sum does not include the spin indices.) Here, N is the number of sites, while β is the inverse temperature in units where Boltzmann's constant is equal to unity. In this low-density limit, we neglect self-energy effects and replace the Green's function by

$$G_0(\mathbf{k},i\omega_n)=\frac{1}{i\omega_n-\varepsilon_{\mathbf{k}}} \tag{5}$$

with the single-particle dispersion relation

$$\varepsilon_{\mathbf{k}}=-2t(\cos k_x a+\cos k_y a)-\mu\ , \tag{6}$$

where a is the lattice spacing.

Our approximation for the fully reducible vertex Eq. (2) obeys the antisymmetry relations

$$\Gamma(1,2;3,4)=-\Gamma(2,1;3,4)=-\Gamma(1,2;4,3)\ . \tag{7}$$

The fully reducible particle-hole vertex which we will use is defined by using crossing relations, namely,

$$\Gamma_{\text{ph}}(1,2;3,4)=-\Gamma(1,3;2,4)=-\Gamma_{\text{ph}}(3,2;1,4)\ . \tag{8}$$

In terms of our approximation for the fully reducible vertex Eq. (2), we have explicitly

$$\Gamma_{\text{ph}}(1,2;3,4)=T(1+3 \text{ or } 2+4)\delta_{1,\bar{3}}(\delta_{1,2}\delta_{3,4}-\delta_{1,4}\delta_{3,2}) \tag{9}$$

again with δ functions on spin only in this expression. This vertex is illustrated in Fig. 2.

This set of equations completely defines our approximation. Note that it is not conserving, except for some special cases ($\mathbf{q}=0$ finite-frequency susceptibilities) which are discussed in Appendix A where we give the Ward identifies for the Hubbard model. One can see that our approach is not conserving more simply by noting that in conserving approximations the irreducible particle-hole vertex is obtained from a functional derivative of the self-energy[1] and here the self-energy vanishes. Note, however, that the full vertex does conserve total crystal momentum, as can be seen from the δ function in the T-matrix definition Eq. (3). The full vertex is also invariant under global spin rotation as may be checked from Eq. (9): it suffices to note that $\delta_{1,\bar{3}}$ is superfluous because of the other combination of δ functions to be able to use the unitarity of the rotation matrices and show that the form

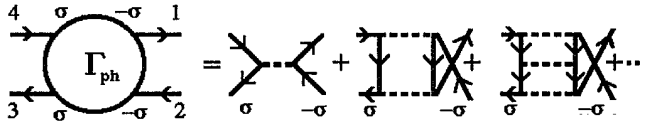

FIG. 2. Definition of the particle-hole fully reducible vertex in our approximation.

of the vertex is the same in the globally rotated frame. Finally, notice that the only momentum dependence of the fully reducible vertex, Eq. (2), is on the total momentum of the incoming or outgoing pairs. Hence, in our approximation, triplet pairs are unaffected by interactions because of their antisymmetry in relative momentum. For singlet pairs with zero total momentum, on the other hand, the only pair correlation functions which are affected by interactions are those which transform according to the fully symmetric representation[18] (A_{1g}) of the group. (s and extended-S pair correlation functions are examples.)

III. COMPARISONS WITH MONTE CARLO SIMULATIONS

To check the validity of our approach, we have performed determinantal Monte Carlo simulations[19] on the two-dimensional nearest-neighbor Hubbard model. We consider separately the particle-hole and particle-particle channels. In all the plots, we work in units where $\hbar=1$, the lattice spacing a is unity, and the hopping parameter t in Eq. (6) is unity. Measurements are done at each time slice. In every other update of the full space-time lattice, no measurement is taken. Time slices are generally of width $\Delta\tau=\frac{1}{10}$ for 4×4 lattices, and of width $\Delta\tau=\frac{1}{8}$ for 8×8 lattices, corresponding to a systematic error due to Trotter splitting which is of the order of the statistical error. Measurements are grouped in blocks to avoid correlations in the estimate of the statistical error.

Even at the lowest densities we study, namely, $\langle n\rangle=0.2$, the Fermi energy measured from the bottom of the band is equal, in the parabolic approximation, to $2\pi\langle n\rangle t\approx1.3t$ which is much larger than the highest temperature we consider, namely, $T\approx0.2t$. For small systems, one also reaches the zero-temperature limit relatively soon because of the discreteness of the spectrum. In 4×4 systems, this happens around $T=t/8$. We have checked that our results still apply in this zero temperature limit.

A. Particle-hole channel

It is useful to define the Fourier transform of the charge and the spin densities as follows:

$$\rho_{\mathbf{q}}=\frac{1}{\sqrt{N}}\sum_{\mathbf{k},\sigma}c^{\dagger}_{\mathbf{k},\sigma}c_{\mathbf{k}+\mathbf{q},\sigma}=\rho_{\mathbf{q}\uparrow}+\rho_{\mathbf{q}\downarrow} \tag{10}$$

for the charge, and

$$S^{z}_{\mathbf{q}}=\frac{1}{\sqrt{N}}\sum_{\mathbf{k},\sigma}\sigma c^{\dagger}_{\mathbf{k},\sigma}c_{\mathbf{k}+\mathbf{q},\sigma} \tag{11}$$

for the spin with $\sigma=\pm1$. The diagrammatic results for particle-hole equal-time correlation functions are computed using the fluctuation-dissipation theorem which, for the charge, for example, takes the form,

$$\langle\rho_{\mathbf{q}}\rho_{-\mathbf{q}}\rangle-\langle\rho_{\mathbf{q}}\rangle\langle\rho_{-\mathbf{q}}\rangle=\int_{-\infty}^{+\infty}\frac{d\omega}{2\pi}\frac{2}{1-e^{-\beta\omega}}\mathrm{Im}[\chi_{\rho\rho}(\mathbf{q},\omega+i\eta)]\ . \tag{12}$$

As usual, η is a positive infinitesimal. The explicit form of our expression for the susceptibility χ is given by

$$\chi_r(1)=\chi_0(1)-\frac{2\sigma_r}{\beta^2N^2}\sum_{2,3}G(2)G(2+1)T(3+1+2)\times G(3)G(3+1)\ , \tag{13}$$

where the index r stands for either spin (zz) or charge ($\rho\rho$) and $\sigma_r=+1$ for density while $\sigma_r=-1$ for spin. The first term is the noninteracting susceptibility and is defined in Appendix B. Here it is the longitudinal spin susceptibility which is computed, but one can check that the expression for the transverse spin susceptibility $\chi_{\pm}$ comes purely from the crossed particle-hole channel and gives the same result (global rotation invariance).

The T matrix has been used previously[10] as the particle-hole *irreducible* vertex to compute magnetic correlations. This generates maximally crossed ladder diagrams and was used to justify the GRPA with renormalized U approach.[10] In the *present* approximation, we consider the T matrix as the *fully* reducible vertex, even though it is irreducible in the particle-hole channel. We are thus in a sense keeping only the first term of the series which would be generated if the T matrix was taken as the irreducible vertex. This is commented upon further in Appendix C.

As a first test of the accuracy of our approximation, consider the following identity between the spin and charge equal-time correlation functions in a paramagnetic phase:

$$I_{\mathbf{q}}\equiv\tfrac{1}{2}\{\langle S^{z}_{\mathbf{q}}S^{z}_{-\mathbf{q}}\rangle+\langle\rho_{\mathbf{q}}\rho_{-\mathbf{q}}\rangle-\langle\rho_{\mathbf{q}}\rangle\langle\rho_{-\mathbf{q}}\rangle\}=2\{\langle\rho_{\uparrow\mathbf{q}}\rho_{\uparrow-\mathbf{q}}\rangle-\langle\rho_{\uparrow\mathbf{q}}\rangle\langle\rho_{\uparrow-\mathbf{q}}\rangle\}\ . \tag{14}$$

We evaluate the left-hand side using the Monte Carlo simulations. In our approximation one can see that this combination of correlation functions should give the same result as that for the noninteracting problem. [Indeed, using Eqs. (12) and (13) on the left-hand side, the interaction disappears; alternatively one can see that the right-hand side reduces to the free case since we assume the vanishing of both self-energy corrections and fully reducible vertex Eq. (9) for parallel-spin particle-hole pairs.] Figure 3 shows the results of the comparison. Even for fillings as high as 0.6, the comparison is excellent. On the other hand, one should note that this test is not too stringent because even when the right-hand side of Eq. (14) is evaluated for the noninteracting problem and the left-hand side is evaluated for the interacting problem, both sides become exactly equal when the sum over $\mathbf{q}$ is performed. This may be proven by transforming to position space and using $n_{\uparrow i}n_{\uparrow i}=n_{\uparrow i}$.

A more detailed comparison of both the spin-spin and charge-charge correlation functions, as calculated from our approximation [Eqs. (12) and (13)] appears in Fig. 4. We introduced the additional approximation of keeping only the zero-frequency part of the fully reducible vertex, as discussed in Appendices B and C. The noninteracting case is also shown in the figure to make the effect of interactions more explicit. We obtain better than 10% accuracy even up to roughly quarter-filling ($\langle n\rangle=0.5$) and

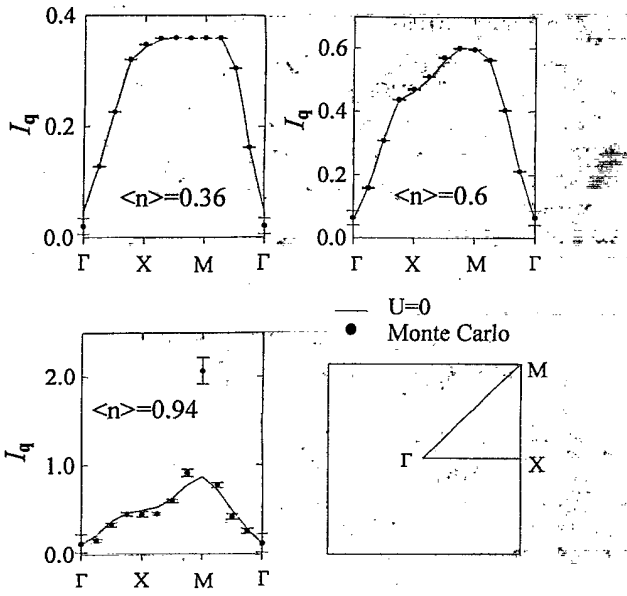

FIG. 3. One-half of the sum of spin and charge correlation functions I_q [see Eq. (14)] for $U=4$, $\beta=5$, and an 8×8 lattice as q moves along the path in the Brillouin zone shown in the bottom right-hand figure. The Monte Carlo results represent an average over 6000 to 10 000 measurements. These Monte Carlo data are the same as those used to plot the following figure. Within our approximation for the vertex, this sum of correlation functions obtained at finite U with the Monte Carlo simulations should equal the $U=0$ results.

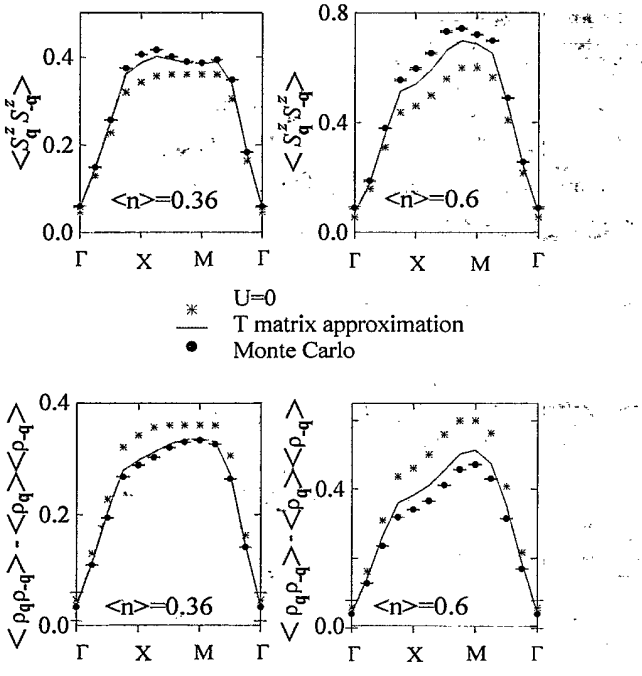

FIG. 4. The first two frames are results for the spin $\langle S_q^z S_{-q}^z \rangle$ correlation function (magnetic structure factor), the last two for the charge $\{\langle \rho_q \rho_{-q} \rangle - \langle \rho_q \rangle \langle \rho_{-q} \rangle\}$ correlation function (charge structure factor) as a function of $\mathbf{q}$, for $U=4$, $\beta=5$, and an 8×8 lattice. Both the T-matrix and the $U=0$ results are calculated for the same 8×8 lattice at the same temperature $\beta=5$. These Monte Carlo data are the same as those used to plot the previous figure.

the agreement is of the same order for both spin and charge. Notice also that the maximum of the interacting system is in general displaced from that in the noninteracting one and that our approximation is able to reproduce this qualitative change, which is the signature of incipient pseudonesting[20] at an incommensurate wave vector. One can remark that the quantitative agreement is here, in general, worse than it was for the sum of the spin and charge correlation functions Eq. (14).

Further verifications of the domain of applicability of this approach can be made. For example, we checked the positivity criterion $\omega\chi_r''(\mathbf{q},\omega)\geq 0$, for the imaginary part $\chi_r''(\mathbf{q},\omega)$ of the dynamical susceptibility, Eq. (13). This condition must be valid for all $\mathbf{q}$ and ω to ensure stability, and we found that it is valid in the regime of interest to us, that is up to intermediate coupling, low temperature, and up to quarter-filling. As expected from Eq. (13), difficulties show up when the interaction U is increased. For example, for $U=10t$ and $\langle n \rangle = 0.6$, positivity of the density is no more ensured, showing that the present approach fails in the strong-coupling regime. The domain of applicability is even smaller for attractive potentials since the positivity criterion for the magnetic channel is no longer satisfied for most band fillings, even in the nonsuperconducting phase.

B. Particle-particle channel

The more widely studied particle-particle correlation functions in the context of high-temperature superconductivity are the equal-time autocorrelation functions $\langle \Delta_\alpha^\dagger \Delta_\alpha \rangle$ for the d-wave and extended-S-wave order parameters. These order parameters are defined by

$$\Delta_\alpha^\dagger = \frac{1}{2\sqrt{N}} \sum_{i,\nu} g^\alpha(\nu) c_{i\uparrow}^\dagger c_{i+\nu\downarrow}^\dagger , \tag{15}$$

where the sum over ν runs over the neighboring sites of i. The value of the weight function $g^\alpha(\nu)$ determines the orbital (s, extended $s,d,p,\ldots$) and spin (triplet or singlet) symmetry of the pair. For singlet order parameters, the weight function is even in space, $g^\alpha(\nu)=g^\alpha(-\nu)$, and the allowed spatial symmetries we consider are

$$\begin{aligned} &s: && g^s(\nu)=\delta_{\nu,0}, \\ &\text{extended } s \text{ (noted } S\text{):} && g^S(\nu)=\delta_{\nu,\hat{x}}+\delta_{\nu,-\hat{x}}+\delta_{\nu,\hat{y}}+\delta_{\nu,-\hat{y}} \\ &d: && g^d(\nu)=\delta_{\nu,\hat{x}}+\delta_{\nu,-\hat{x}}-\delta_{\nu,\hat{y}}-\delta_{\nu,-\hat{y}}. \end{aligned} \tag{16}$$

For triplet order parameters the weight function is odd in space, $g^\alpha(\nu)=-g^\alpha(-\nu)$, and the spatial symmetry we consider is p_x ($S_z=0$ component), namely, $g^{p_x}(\nu)=\delta_{\nu,\hat{x}}-\delta_{\nu,-\hat{x}}$. It is also convenient to work in Fourier space,

$$\Delta_\alpha^\dagger = \frac{1}{2\sqrt{N}} \sum_{\mathbf{k}} F^\alpha(\mathbf{k}) c_{\mathbf{k}\uparrow}^\dagger c_{-\mathbf{k}\downarrow}^\dagger , \tag{17}$$

where

$$F^\alpha(\mathbf{k}) = \sum_\nu g^\alpha(\nu) e^{i\mathbf{k}\cdot\mathbf{x}_\nu} . \tag{18}$$

As usual, for an extended-S wave we have $F^{\alpha}(\mathbf{k})=F^{s}(\mathbf{k})=2[\cos(k_x)+\cos(k_y)]$, for a d wave $F^{d}(\mathbf{k})=2[\cos(k_x)-\cos(k_y)]$, and for a p_x wave $F^{p}(\mathbf{k})=2i\sin(k_x)$. These form factors are orthogonal when integrated over the whole Brillouin zone. For form factors orthogonal on the Fermi surface, other definitions are more appropriate[21] but we shall not consider these here. Extensive Monte Carlo studies have been done to determine the more likely shape of the order parameter[22] including some work with finite center-of-mass momentum.[23] We do not explore all these possibilities. The aim is rather to see if the T-matrix approximation can account for pair correlation functions as well as it did in the crossed magnetic and density channels. No superconductivity is expected in the low-density regime of interest here. Because in the T-matrix formalism only particles with different spins interact, the fully reducible vertex is nonzero only for certain singlet pair correlation functions. Triplet pair correlation functions will not differ from their $U=0$ value.

Just as for particle-hole correlation functions, pair correlation functions can be related to the corresponding susceptibilities. One must be careful that because of the anticommunication relations, there is, in general, a difference between $\langle\Delta_\alpha^\dagger\Delta_\alpha\rangle$ and $\langle\Delta_\alpha\Delta_\alpha^\dagger\rangle$.[22] Pair correlation functions are obtained here from the appropriate fluctuation-dissipation theorem,

$$\langle\Delta_\alpha^\dagger\Delta_\alpha\rangle=\int_{-\infty}^{+\infty}\frac{d\omega}{2\pi}\frac{2}{1-e^{-\beta\omega}}\mathrm{Im}[\chi_\alpha(\mathbf{q}=0,\omega+i\eta)]\ . \tag{19}$$

The pair susceptibility is defined by

$$\chi_\alpha(\mathbf{q}=0,\omega+i\eta)=\int_{-\infty}^{\infty}\frac{d\omega'}{\pi}\frac{\chi''_\alpha(\omega')}{\omega'-\omega-i\eta}\ , \tag{20}$$

where

$$\chi''_\alpha(t)=\tfrac{1}{2}\langle[\Delta_\alpha^\dagger(t),\Delta_\alpha(0)]\rangle\ . \tag{21}$$

The imaginary part of the susceptibility can appear in the kernel of the integral in (19) because the quantity defined in Eq. (21) satisfies $\chi''_\alpha(t)=[\chi''_\alpha(-t)]^*$.

In the triplet channels, interactions do not come in and the susceptibility is simply

$$\chi^0_\alpha(1)=\frac{1}{4\beta N}\sum_2 F^{\alpha}(2)[F^{\alpha}(2)]^*G(2-1)G(-2)\ . \tag{22}$$

Note that here and in what follows, the index 1 on the left-hand side stands for frequency since we study pairing correlations for $\mathbf{q}=0$ only. The fact that the form factors F^{α} do not depend on frequency allows simplified arguments to occur in (22). In Fig. 5 we plot the p-wave correlation function as a function of doping. The solid line represents the T-matrix prediction, which is the same as the noninteracting result. Clearly, the Monte Carlo data deviate from the T-matrix prediction only for fillings of order 0.6 and larger. Note also that close to half-filling, the correlations are reduced compared with the noninteracting case.

The expression for the pair susceptibility in singlet channels is given by

$$\chi_\alpha(1)=\chi^0_\alpha(1)-\frac{1}{4\beta^2N^2}\sum_{2,3}F^{\alpha}(2)F^{\alpha}(3)G(2-1)G(-2)T(-1)G(3-1)G(-3)\ . \tag{23}$$

Since the indices 2 and 3 do not enter the T matrix in the equation for the susceptibility (23), the two sums may be factored. After performing the Matsubara frequency sums, the expression takes the form

$$\chi_\alpha(\mathbf{q}=0,i\omega_q)=\frac{1}{4N}\sum_{\mathbf{k}}[F^{\alpha}(\mathbf{k})]^2\frac{1-2f(\varepsilon_{\mathbf{k}})}{2\varepsilon_{\mathbf{k}}+i\omega_q}-\frac{U}{1+U\chi_{pp}(0,i\omega_q)}\left\{\frac{1}{2N}\sum_{\mathbf{k}}F^{\alpha}(\mathbf{k})\frac{1-2f(\varepsilon_{\mathbf{k}})}{2\varepsilon_{\mathbf{k}}+i\omega_q}\right\}^2\ , \tag{24}$$

where the sum of ladder diagrams defined in Eq. (4) is given by

$$\chi_{pp}(0,i\omega_q)=\frac{1}{N}\sum_{\mathbf{k}}\frac{1-2f(\varepsilon_{\mathbf{k}})}{2\varepsilon_{\mathbf{k}}+i\omega_q}\ . \tag{25}$$

We now study the various cases in turn.

1. *d wave [B_{2g} symmetry (Ref. 18)]*

This particular symmetry, combined with the lattice symmetry of the energy spectrum, makes the term in curly brackets in Eq. (24) cancel. An analytical continuation and a frequency integration then lead to the simple result

$$\langle\Delta_d^\dagger\Delta_d\rangle=\frac{1}{N}\sum_{\mathbf{k}}(\cos k_x-\cos k_y)^2f^2(\varepsilon_{\mathbf{k}})\ . \tag{26}$$

Thus, in the T-matrix approximation, $\langle\Delta_d^\dagger\Delta_d\rangle$ is explicit-

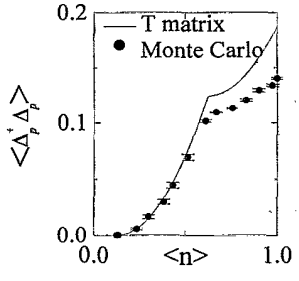

FIG. 5. Triplet pair correlation function $\langle\Delta_p^\dagger\Delta_p\rangle$ plotted as a function of filling for $U=4$, $\beta=6$, on a 4×4 lattice. The T-matrix result is the same as the $U=0$ result and is calculated on the same 4×4 lattice at the same temperature $\beta=6$. The Monte Carlo results represent an average over 3×10^4–10^6 measurements.

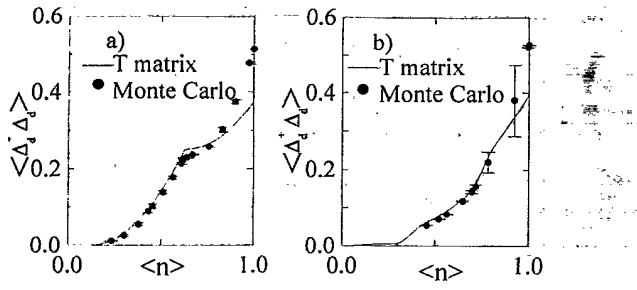

FIG. 6. Singlet d-wave correlation function $\langle \Delta_d^\dagger \Delta_d \rangle$ plotted as a function of filling for $U=4$, $\beta=6$. The T-matrix result is the same as the $U=0$ result and is calculated on the same lattice sizes at the same temperature $\beta=6$. The Monte Carlo results represent an average over 3×10^4–10^6 measurements: (a) 4×4 lattice, (b) 8×8 lattice.

ly independent of the interaction strength. For a moderate U, this is accurate not too close to half-filling as can be seen in Fig. 6, where Monte Carlo results for $U=4t$ have been plotted. These calculations were done for 4×4 and 8×8 lattices and $\beta t=6$. The point where a discontinuity in the slope occurs is a finite-size effect and has also been observed in the chemical potential. It corresponds to an integer number of electrons on the lattice. If U/t is increased (for example, $U=10t$), the same level of accuracy is maintained only for lower fillings (until roughly $\langle n \rangle=0.4$). These results are consistent with those of Moreo and Scalapino[22] who studied in detail various pair-field symmetries to isolate the role of the vertex from self-energy effects. They compared the pair correlation functions and the corresponding nonvertex part of the same correlation functions obtained by Monte Carlo simulations. For d-wave symmetry they found a sizable difference between these two only near half-filling. Vertex effects were unnoticeable for lower fillings, as can also be seen from Fig. 6. Thus, for a wide range of band fillings, d-wave pair-field correlations are unaffected by either effective interaction or quasiparticle-renormalization effects.

Although we did not show this in the figure, the T-matrix result for 40×40 lattices is not very different from the 8×8 case. As can be seen from Fig. 6, however, very sizable finite-size effects exist for 4×4 systems, and this is true in all cases we have looked at. It seems however, that the order of magnitude of these effects is determined mostly by the noninteracting case. It is important to perform the T-matrix calculation for the same system size as the Monte Carlo simulation.

2. *s and S pairings [A_{1g} symmetry (Ref. 18)]*

For these orbital states the second term appearing on the right-hand side of (24) no longer cancels and interactions contribute to the pair correlation function. Performing the analytical continuation $i\omega_q \rightarrow \omega+i\eta$ and taking the limit $\eta\rightarrow0$ for $\chi_{s(S)}(\mathbf{q}=0,\omega+i\eta)$ requires some care: for finite systems, this cannot be done independently in the bracket and in the denominator $[1+U\chi_{pp}(0,\omega+i\eta)]$ appearing in Eq. (24). To do the frequency integration over the imaginary part of the susceptibility, as required to obtain $\langle \Delta_{s(S)}^\dagger \Delta_{s(S)} \rangle$, one must locate numerically all the poles of the susceptibility and then perform a sum over the δ functions located at each pole. Indeed, the result of the analytical continuation for the imaginary part of $\chi_{s(S)}$ is a Dirac comb, as for the $U=0$ case, except that for $U\neq0$ the δ functions' arguments are displaced. The poles stay in a one-to-one correspondence with the noninteracting case where they were located at $\omega+2\varepsilon_k=0$. Two of these poles are found, respectively, below and above the two-hole continuum, which is bounded by $\min(-2\varepsilon_k)$ and $\max(-2\varepsilon_k)$ when the total momentum of the pair is zero. The upper pole has the same physical origin[24] as the one first reported in two-dimensional jellium by Engelbrecht and Randeria.[9] The other pole is a two-electron antibound state[25] which appears because of the finite band. For a finite system, all the poles, including the latter two collective modes, are on the same footing and hence they do not require special treatment. We only need to be careful to include all of them. At zero temperature, note that the two-electron antibound state does not contribute to the frequency integral leading to the equal-time correlation function.

For the S wave, the results appear in Fig. 7. Monte Carlo results and those of the T-matrix approximation are given as a function of filling. The noninteracting case is also plotted. Comparing it with the T-matrix results, we note that the interactions act in opposite ways depending on filling: At low density, the vertex reduces correlations, whereas it increases them at higher density, as if the effective interaction was attractive. For fillings larger than $\langle n \rangle \approx 0.6$ this effective attractive interaction is sizable. The T-matrix approximation reproduces the Monte Carlo results over the whole range of band fillings, including the saturation regime at high filling. There is only a slight overestimation. The effective attractive interaction was also observed by Moreo and Scalapino[22] when comparing correlation functions with and without vertex part.

Pair-field correlation functions in a way measure the correlations that exist between two-quasiparticle hops:

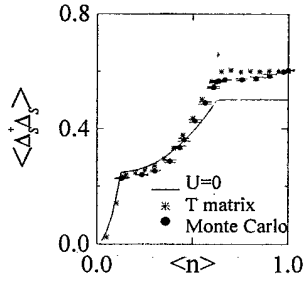

FIG. 7. Singlet extended-S-wave correlation function $\langle \Delta_S^\dagger \Delta_S \rangle$ plotted as a function of filling for $U=4$, $\beta=6$, and a 4×4 lattice. Both the T-matrix result and the $U=0$ results are calculated for the same 4×4 lattice at the same temperature $\beta=6$. The Monte Carlo results represent an average over 3×10^4–10^6 measurements.

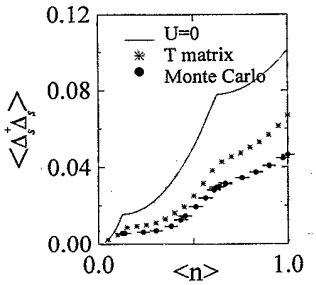

FIG. 8. Singlet s-wave correlation function $\langle \Delta_s^\dagger \Delta_s \rangle$ plotted as a function of filling for $U=4$, $\beta=6$, on a 4×4 lattice. Both the T-matrix result and the $U=0$ results are calculated for the same 4×4 lattice at the same temperature $\beta=6$. The Monte Carlo results represent an average over $3\times10^4-10^6$ measurements.

one hop is from a site l to another site l', the other hop is from a neighboring site of l to a neighboring site of l'. Thus, it may appear that a nonlocal effective interaction (like paramagnons) would have a stronger influence on the correlations of these jumps than a local interaction. Surprisingly, the T-matrix approximation, which remains a local effective interaction, gives by itself a satisfactory account of these types of correlations in the low-density limit. This is completely consistent with previous studies[26] which explicitly showed that S-wave correlations have very short range, making their enhancement compared to the noninteracting case irrelevant for superconductivity.

The local s correlation function is also of interest. In the one-band Hubbard model, a theorem due to Zhang[27] relates extended S and local s order parameters, probably preventing S superconductivity because s order is unlikely due to local repulsion. Results for the s-pair channel are plotted in Fig. 8. Correlations are strongly depressed over the whole range of band filling, compared to the noninteracting case. The T-matrix approximation goes in the same direction but is not enough to decrease the correlations sufficiently at large filling. Note, however, that these correlations are already small and hence probably hard to obtain quantitatively.

IV. CONCLUSION

Equal-time correlation functions in all channels compare very well with Monte Carlo simulations in the low-density, ($\langle n \rangle < 0.5$) intermediate-coupling ($U \sim 4t$) limit when the fully reducible vertex is approximated by the T matrix in a crossing-symmetric manner. This approach is much simpler than either conserving[1,2] or parquet[5] approaches, is physically clear, and accounts for most of the effect of interaction in all channels and for quite a wide range of parameters. The importance of this result, however, lies not so much in the explanation of the Monte Carlo data as in the fact that it shows that nontrivial effects coming from paramagnon or from strong-coupling effects occur in Monte Carlo simulations only close to half-filling or for values of the repulsion U much larger than those usually studied, which are somewhat less than the bandwidth. Our results also show that at low density, and in the range of coupling most widely studied in Monte Carlo simulations, the two-dimensional Hubbard model can most likely be described by a weakly correlated Fermi liquid, as explained further in Appendix C. This also sheds light on the renormalized GRPA approach to magnetic correlations proposed previously.[10–12]

As far as pairing correlations are concerned, it is also noteworthy that close to half-filling the increase seen in the d-wave channel by Monte Carlo simulations cannot be accounted for by T-matrix effects. By contrast, in the extended-S channel, the T-matrix essentially accounts for everything. Antiparamagnon theories would suggest that the additional correlations in the d-wave channel are related to those also seen in the magnetic channel.

ACKNOWLEDGMENTS

We would like to thank Pierre Bénard, Claude Bourbonnais, René Côté, Daniel Groleau, David Sénéchal, and Yury Vilk for comments and for useful conversations. We are also grateful to Daniel Groleau for permission to use data from his M.Sc. thesis in Appendix C, and to P.C.E. Stamp for pointing out Ref. 6. A. Reid, C. Boily, and H. Nélisse have contributed to set up the Monte Carlo program. We acknowledge the support of the Natural Sciences and Engineering Council of Canada (NSERC), the Fonds pour la formation de Chercheurs et l'aide à la recherche from the Government of Québec (FCAR), and (A.-M.S.T.) the Canadian Institute of Advanced Research (CIAR).

APPENDIX A: WARD IDENTITIES FOR LATTICE ELECTRONS

The Ward identities for lattice electrons look somewhat different from the usual ones, although they are derived using the standard approach. We quote these identities for reference and also because one can see explicitly that the main approximation in the present paper violates them, except for special cases.

First note that both charge and spin are locally conserved quantities. Both can be combined in a shorthand notation by defining the 2×2 matrices σ^μ, with σ^0 equal to the identity matrix and σ^i equal to the Pauli spin matrices σ^x, σ^y, σ^z, for $i=1,2,3$, respectively. Define the Fourier transform of the local charge and spin densities by

$$\rho_{\mathbf{q}}^\mu = \frac{1}{\sqrt{N}} \sum_{\mathbf{k},\alpha\beta} c_{\mathbf{k},\alpha}^\dagger \sigma_{\alpha\beta}^\mu c_{\mathbf{k}+\mathbf{q},\beta} = \frac{1}{\sqrt{N}} \sum_{\mathbf{k}} \mathbf{c}_{\mathbf{k}}^\dagger \sigma^\mu \mathbf{c}_{\mathbf{k}+\mathbf{q}} \,. \quad \text{(A1)}$$

The last expression introduces a matrix notation. One can derive the following local conservation law for electrons having a general (arbitrary-neighbor hopping) one-band dispersion relation $\varepsilon_{\mathbf{k}}$:

$$\frac{\partial \rho_{\mathbf{q}}^\mu}{\partial \tau} = -\frac{1}{\sqrt{N}} \sum_{\mathbf{k}} (\varepsilon_{\mathbf{k}+\mathbf{q}} - \varepsilon_{\mathbf{k}}) \mathbf{c}_{\mathbf{k}}^\dagger \sigma^\mu \mathbf{c}_{\mathbf{k}+\mathbf{q}} \,. \quad \text{(A2)}$$

All operators above are assumed to be at the same imaginary time τ. This result applies not only to the Hubbard model but also to any one-band Hamiltonian whose interaction part commutes with the local charge and spin operators. Even though this is not obvious from Eq. (A2), the right-hand side does correspond to the appropriate discrete generalization of the divergence of the current operator. The Ward identities relate four-point correlation functions and Green's functions defined, respectively, as follows:

$$\Lambda^{\mu,\nu}(\mathbf{k}\tau,\mathbf{k}+\mathbf{q}\tau;\mathbf{k}'+\mathbf{q}\tau_1,\mathbf{k}'\tau_2) = \langle T_\tau c^\dagger_{\mathbf{k}}(\tau)\sigma^\mu c_{\mathbf{k}+\mathbf{q}}(\tau)c^\dagger_{\mathbf{k}'+\mathbf{q}}(\tau_1)\sigma^\nu c_{\mathbf{k}'}(\tau_2)\rangle \ , \quad \text{(A3)}$$

$$\mathbf{G}_{\mathbf{k}}(\tau_1-\tau_2) = -\langle T_\tau \mathbf{c}_{\mathbf{k}}(\tau_1)\mathbf{c}^\dagger_{\mathbf{k}}(\tau_2)\rangle \ . \quad \text{(A4)}$$

As usual T_τ is the time-ordered-product operator and $\mathbf{G}_{\mathbf{k}}$ is a 2×2 matrix in spin space.

Letting Tr denote a trace over spin indices, the Ward identities may now be written explicitly:

$$\sum_{\mathbf{k}} \left[\frac{\partial \Lambda^{\mu\nu}}{\partial \tau} + (\varepsilon_{\mathbf{k}+\mathbf{q}}-\varepsilon_{\mathbf{k}})\Lambda^{\mu\nu} \right] = \delta(\tau-\tau_1)\mathrm{Tr}[\mathbf{G}_{\mathbf{k}'}(\tau_2-\tau)\sigma^\mu\sigma^\nu] - \delta(\tau-\tau_2)\mathrm{Tr}[\mathbf{G}_{\mathbf{k}'+\mathbf{q}}(\tau-\tau_1)\sigma^\nu\sigma^\mu] \ . \quad \text{(A5)}$$

Since in our problem there is no spin-orbit interaction and we are in the paramagnetic phase, the system is rotationally invariant in spin space. This means that $\mathbf{G}_{\mathbf{k}}$ is proportional to the identity matrix, and that the tensor $\Lambda^{\mu\nu}$ is diagonal, with two independent components only, Λ^{00} and Λ^{ii} (independent of i, and different from each other when the interaction is nonzero). The right-hand side of this last equation can then be simplified further by using trace identities for the Pauli matrices. The fact that there are just two independent Ward identities in our problem is easy to understand by noticing that the functional form of the Hamiltonian implies that the number of spin-up electrons and the number of spin-down electrons are separately conserved, corresponding to two independent conservation laws.

Note that if one sets τ_1 equal to τ_2, then the right-hand side of Eq. (A5) vanishes when $\mathbf{q}=0$. Leaving the Matsubara frequency corresponding to $\mathbf{q}$ different from zero, and summing over $\mathbf{k}'$, one then easily sees from Eq. (A5) that this proves that the finite-frequency charge or spin susceptibilities vanish at $\mathbf{q}=0$. This is a well-known fact which follows from the global conservation laws. In the case where the frequency dependence of the T matrix is neglected, our approximation also satisfies this requirement, as can be seen by using the explicit expressions in Appendix B.

APPENDIX B: PARTICLE-HOLE CORRELATION FUNCTIONS

To make the evaluation of the charge and spin correlation functions more tractable, we introduce one further approximation, namely that the fully reducible vertex Γ appearing in Eq. (13) can be approximated by its value at zero Matsubara frequency. This is a physically motivated approximation often used in paramagnon[6] or induced-interaction[28] theories, for example. It is also consistent with Fermi-liquid ideas[29] according to which all particles that scatter are very close to the Fermi surface. With this approximation, the sums over Matsubara frequencies can be performed to obtain, from Eq. (13),

$$\chi_r(q) = -\frac{2}{N}\sum_{\mathbf{k}} \frac{f(\varepsilon_{\mathbf{k}})-f(\varepsilon_{\mathbf{k}+\mathbf{q}})}{\varepsilon_{\mathbf{k}}-\varepsilon_{\mathbf{k}+\mathbf{q}}+i\omega_q} - \frac{2\sigma_r}{N^2}\sum_{\mathbf{k},\mathbf{k}'} \frac{f(\varepsilon_{\mathbf{k}})-f(\varepsilon_{\mathbf{k}+\mathbf{q}})}{\varepsilon_{\mathbf{k}}-\varepsilon_{\mathbf{k}+\mathbf{q}}+i\omega_q} T(\mathbf{k}+\mathbf{q}+\mathbf{k}',0) \times \frac{f(\varepsilon_{\mathbf{k}'})-f(\varepsilon_{\mathbf{k}'+\mathbf{q}})}{\varepsilon_{\mathbf{k}'}-\varepsilon_{\mathbf{k}'+\mathbf{q}}+i\omega_q} \ . \quad \text{(B1)}$$

The first term on the right-hand side is the zeroth-order Lindhard function χ_0 appearing in Eq. (13). Also, r stands for either charge or spin and $\sigma_r=+1$ for density while $\sigma_r=-1$ for spin. In performing the analytical continuation to compute the imaginary part, the case $\varepsilon_{\mathbf{k}}-\varepsilon_{\mathbf{k}+\mathbf{q}}=\varepsilon_{\mathbf{k}'}-\varepsilon_{\mathbf{k}'+\mathbf{q}}$ needs to be handled separately. In fact, the double pole does not lead to unphysical results only because an integral over frequency is performed. For a susceptibility this double pole would not be physical, as can be checked from the Lehmann representation. Integrating the imaginary part with the appropriate Bose factor [Eq. (12)] to obtain the correlation functions, we find

$$\langle S^Z_{\mathbf{q}} S^Z_{-\mathbf{q}}\rangle = S_0 - S_1 - S_2 \ , \quad \text{(B2)}$$

$$\langle \rho_{\mathbf{q}}\rho_{-\mathbf{q}}\rangle - \langle \rho_{\mathbf{q}}\rangle\langle \rho_{-\mathbf{q}}\rangle = S_0 + S_1 + S_2 \ , \quad \text{(B3)}$$

where

$$S_0 = \frac{2}{N}\sum_{\mathbf{k}} f(\varepsilon_{\mathbf{k}})[1-f(\varepsilon_{\mathbf{k}+\mathbf{q}})] \ , \quad \text{(B4)}$$

$$S_1 = -\frac{4}{N^2}\sum_{\mathbf{k},\mathbf{k}'}^{(1)} \frac{\{f(\varepsilon_{\mathbf{k}})[1-f(\varepsilon_{\mathbf{k}+\mathbf{q}})]\}\{f(\varepsilon_{\mathbf{k}'})-f(\varepsilon_{\mathbf{k}'+\mathbf{q}})\}}{\varepsilon_{\mathbf{k}}-\varepsilon_{\mathbf{k}+\mathbf{q}}-\varepsilon_{\mathbf{k}'}+\varepsilon_{\mathbf{k}'+\mathbf{q}}} \times T(\mathbf{k}+\mathbf{k}'+\mathbf{q},0) \ , \quad \text{(B5)}$$

$$S_2 = -\frac{2\beta}{N^2}\sum_{\mathbf{k},\mathbf{k}'}^{(2)} \{f(\varepsilon_{\mathbf{k}})[1-f(\varepsilon_{\mathbf{k}+\mathbf{q}})]\}\{[1-f(\varepsilon_{\mathbf{k}'})]f(\varepsilon_{\mathbf{k}'+\mathbf{q}})\} \times T(\mathbf{k}+\mathbf{k}'+\mathbf{q},0) \ , \quad \text{(B6)}$$

and where the sums $\sum^{(1)}_{\mathbf{k},\mathbf{k}'}$ and $\sum^{(2)}_{\mathbf{k},\mathbf{k}'}$ run over values of $\mathbf{k}$ and $\mathbf{k}'$ such that, respectively, $\varepsilon_{\mathbf{k}}-\varepsilon_{\mathbf{k}+\mathbf{q}}-\varepsilon_{\mathbf{k}'}+\varepsilon_{\mathbf{k}'+\mathbf{q}}$ is different from, or equal to, zero.

APPENDIX C: VALIDITY OF GRPA AND RELATION TO FERMI-LIQUID THEORY

In previous work,[10–12] it was argued that good agreement with Monte Carlo simulations for the magnetic structure factor could be obtained by simply using a renormalized value of the Hubbard U in the standard GRPA approach without self-energy corrections. In the low-density limit, the origin of the renormalization of U can be understood from the work of Galitskii,[15] Brueckner,[16] and Kanamori:[17] In this regime, the full T matrix should replace the bare interaction U in the GRPA sum. This was shown by Chen *et al.*[10] by explicitly solving the corresponding integral equations. (We refer to this calculation as MCL, since it is the sum of maximally crossed ladders.) Close to half-filling, the MCL approach becomes less accurate,[10] as discussed further by Bulut and Scalapino.[12] In this appendix, we discuss the relation between the MCL approach and the present paper. We also comment on the relation between the MCL approach, the GRPA with renormalized U approach, and Fermi-liquid theory. It will clearly come out that even at intermediate coupling ($U \sim 4t$), the two-dimensional Hubbard model in the low-density limit is accurately described by a weakly correlated Fermi liquid.

Before proceeding, we digress to explain why we call the approach of Refs. 10–12 the GRPA approach instead of the RPA. When the Hubbard Hamiltonian is written out in its standard form, one already takes into account the cancellation between direct and exchange terms for parallel spins interacting through the zero-range potential U. In this case, the RPA approach is equivalent to what would have been obtained from the GRPA if instead the potential part of the Hamiltonian had been written out in the form

$$\frac{U}{2}\sum_{i,\sigma,\sigma'} c_{i\sigma}^{\dagger}c_{i\sigma'}^{\dagger}c_{i\sigma'}c_{i\sigma} .$$

The latter form is explicitly rotationally invariant: this has the advantage that the Baym-Kadanoff arguments[1] immediately imply that when the Hartree-Fock approximation is used for the self-energy, the GRPA (sum of particle-hole ladders and bubbles) is conserving. In terms of diagrams, both the transverse and longitudinal spin susceptibilities are, in this approach, given in terms of the same set of diagrams, namely, particle-hole ladders. This approach can be directly used for a finite-range potential. By contrast, the RPA approach, where bubbles are used for longitudinal susceptibility and ladders for the transverse one, is useful only for the Hubbard model. Rotational invariance is lost for a finite-range potential under any approximation for the self-energy. Again, however, note that what we call GRPA and what is called RPA in Refs. 10–12 are, in fact, here the same approximation because the potential is independent of momentum (zero range in space).

Returning to the main point of this appendix, recall that, as shown in Fig. 1, the spin and charge susceptibilities may be computed from the fully reducible four-point vertex Γ. Following the notation of Fig. 1 and of Refs. 5 and 30, with only minor modifications, we write the integral equation for the fully reducible vertex Γ as a function of an irreducible vertex $\Gamma^{(1)}$ in the following form (in the finite-temperature formalism and with a sum over repeated indices implied):

$$\Gamma(1,2;3,4)=\Gamma^{(1)}(1,2;3,4)+\Gamma^{(1)}(1,2';3',4)G(2')G(3')\times\Gamma(3',2;3,2') . \quad \text{(C1)}$$

The diagrammatic form of this integral equation appears in Fig. 9. We take advantage of momentum conservation to define

$$\Gamma(1,2;3,4)=\Gamma(1,2;2-5,1+5)\equiv\Gamma(1,2:5) , \quad \text{(C2)}$$

where 5 is the momentum transfer. The last notation on the right-hand side has the disadvantage of being ambiguous with spin indices, which do not appear anymore. On the other hand, the notation clarifies the role of the various momenta, and any ambiguity with spin can always be eliminated by returning to the original equation, Eq. (C1), for the fully reducible vertex Γ. This equation can now be written in the following simplified form:

$$\Gamma(1,2:5)=\Gamma^{(1)}(1,2:5)+\Gamma^{(1)}(1,2'+5:5)G(2'+5)G(2')\times\Gamma(2',2:5) . \quad \text{(C3)}$$

$\Gamma^{(1)}$ is the vertex which is irreducible in the ("Landau") particle-hole channel which transports the momentum label 5. Following Galitskii,[15] Brueckner,[16] and Kanamori,[17] we use the T matrix for $\Gamma^{(1)}$ in exactly the manner described in the main part of this paper: parallel-spin electrons do not interact, while for antiparallel spins the full Bethe-Salpeter equation is solved. It should be noted that from a more modern renormalization-group point of view[31] this choice is justified by the fact that, to one-loop order, these T-matrix effects are the only ones which come in when eliminating high-energy degrees of freedom to find the fixed-point theory.

The approximation discussed in the main body of this paper amounts to approximating the full vertex Γ in Eq. (C3) by the first term of the infinite series, namely, $\Gamma^{(1)}$

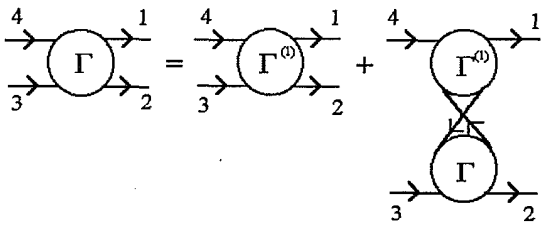

FIG. 9. Integral equation for the fully reducible vertex Γ in terms of the vertex $\Gamma^{(1)}$ which is irreducible in the Landau channel. This integral equation is used in the microscopic derivation of Landau Fermi-liquid theory.

($\Gamma^{(1)}$ being approximated by the T matrix). In Ref. 10, the full series was summed to compute the $\mathbf{q}=0$ magnetic-structure factor.[32] The results of these two approaches are compared in Figs. 10–12. The approach of the present paper is abbreviated by "T matrix" in the caption, while the approach of Ref. 10, which solves the full integral equation, is abbreviated by MCL, which stands for "maximally crossed ladders." First, let us point out that, in all these figures, the oscillations as a function of filling are a finite-size effect.[33] For fillings around roughly $\langle n \rangle = 0.4$, none of the approximations seem to work for both spin and charge, even though any of these approximations is, in general, closer to the Monte Carlo results than the $U=0$ case. By contrast, at low density, all the approximations seem equally good in the figures for the 4×4 lattice (Figs. 10 and 11). One needs to go to the 8×8 lattice (Fig. 12, bottom panel in particular) to see that the solution to the full integral equation (C3) gives a better approximation to the Monte Carlo results than keeping only the first term $\Gamma^{(1)}$. Three further points are worth making: (a) In the regions where the agreement with the Monte Carlo calculation is good, it does not make much difference whether one approximated the T matrix by its zero-frequency value, or if the full Matsubara frequency dependence is taken into account. (b) Keeping only the first term, $\Gamma^{(1)}$, of the series for Γ accounts for most of the correlations which are picked up by summing the full series (MCL). This suggests that at low density and intermediate coupling, the small lattices are very well described by a weakly correlated Fermi liquid, a point on which we elaborate below. (c) Even if keeping only the first term, $\Gamma^{(1)}$, of the series for Γ accounts for most of the correlations, it is clear that this procedure cannot reproduce the zero-sound pole: the collective-mode behavior present in frequency-dependent correlation functions would not be well reproduced by the approach of the present paper.

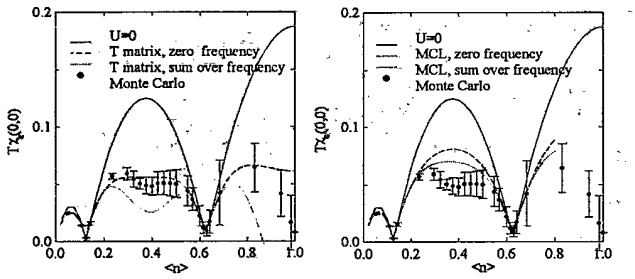

FIG. 10. Uniform charge susceptibility times temperature (or equivalently, static $\mathbf{q}=0$ charge structure factor) as a function of filling factor $\langle n \rangle$, computed for a 4×4 lattice at $\beta=5$. In both parts of the figure, the cases $U=0$ (solid line) as well as the Monte Carlo results (points with error bars) appear. In the left panel, the full vertex Γ is approximated by the T matrix with no self-energy effects, as in the bulk of the present paper. [This can be seen as keeping only the first term of the series for Γ in Eq. (C3), namely, $\Gamma^{(1)}$, and approximating $\Gamma^{(1)}$ by the T matrix.] The dotted line shows the result when the full frequency dependence of the T matrix is taken into account, while in the calculation represented by the long-dashed line, the T matrix is approximated by its zero-frequency value. In addition to the $U=0$ and the Monte Carlo results, the right panel displays the results obtained when the full integral equation (Ref. 32) for the vertex Γ in Eq. (C3) is solved (MCL approach), again replacing $\Gamma^{(1)}$ by the T matrix. As in the left panel, the dotted line shows the result when the full frequency dependence of the T matrix is taken into account, while in the calculation represented by the long-dashed line, the T matrix is approximated by its zero-frequency value.

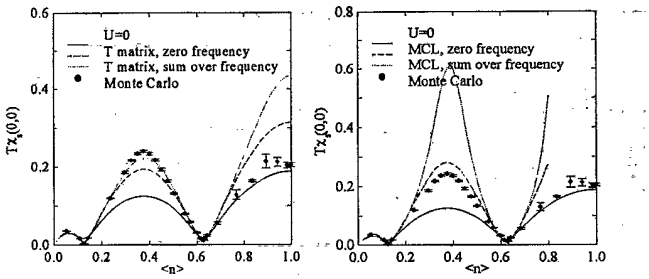

FIG. 11. Symbols and parameters are as in Fig. 10, but this time it is the spin instead of the charge structure factor which is displayed.

It was pointed out in previous work[10] that, at low density, it is not even necessary to solve the full integral equation (MCL). One can replace the T matrix by a renormalized contact interaction U_{rn}, and then use the GRPA approach with this U_{rn}. It was also suggested that this U_{rn} could be computed from a Brillouin-zone average of the zero-frequency T matrix. In the rest of this appendix, we show how the validity of this approach for $\mathbf{k}_5 \rightarrow 0$ follows from microscopic theory for a weakly correlated Fermi liquid.

To make the connection with microscopic Fermi-liquid theory, we start as in Refs. (29) or (30), from Eq. (C3) for the fully reducible vertex Γ in terms of the vertex $\Gamma^{(1)}$ which is irreducible in the "Landau channel." We need to recall a few results from the microscopic approach to Landau Fermi-liquid theory.[29,30] First, the quasiparticle form of the Green's function product takes the form

$$G(2'+5)G(2') \approx a^2 G_0^*(2'+5)G_0^*(2')+\phi(5) , \qquad \text{(C4)}$$

where G_0^* has the functional form of a free-particle Green's function but with a renormalized mass: The quasiparticle weight, normally called Z, here is a, while ϕ is the so-called "incoherent part." Substituting this form of the Green's functions in the integral equation for the vertex (C3), one finds,[29,30] by taking the limit $\mathbf{k}_5 \rightarrow 0$ before the zero-frequency limit, that the corresponding limiting behavior of the vertex, noted Γ^{ω}, is given by

$$\Gamma^{\omega} = (1-\Gamma^{(1)}\phi)^{-1}\Gamma^{(1)} . \qquad \text{(C5)}$$

The Fermi-liquid parameters are then computed from

$$f_{\mathbf{pp}'}^{\uparrow\downarrow} = a^2\Gamma^{\omega} \equiv a^2\Gamma(\mathbf{p},0\uparrow,\mathbf{p}',\omega\downarrow;\mathbf{p}',0\downarrow,\mathbf{p},\omega\uparrow)$$
$$\equiv a^2\Gamma(\mathbf{p},0\uparrow,\mathbf{p}',\omega\downarrow:0,\omega) . \qquad \text{(C6)}$$

The frequency label is zero for a particle at the Fermi surface. Here all particles have their momenta on the

Fermi surface, but they are not on the energy shell.

Suppose that the liquid is weakly correlated, in the sense that $a \approx 1$. Then the frequency sum rule for the spectral weight implies that the incoherent part of the Green's function cannot be large. Taking then $\phi \approx 0$ in the expression (C5) for Γ^{ω}, one finds that the Landau function f is well approximated by

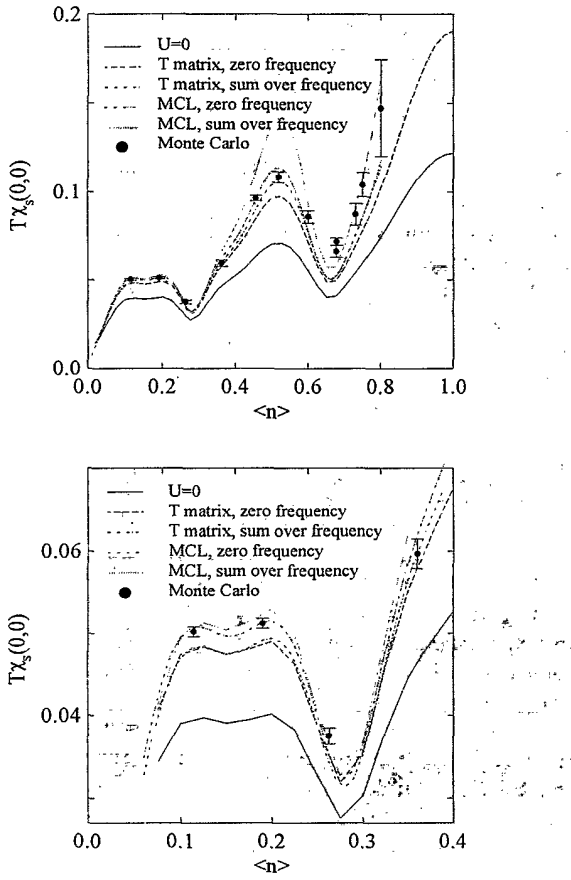

FIG. 12. Uniform spin susceptibility times temperature (or equivalently, static $\mathbf{q}=\mathbf{0}$ spin structure factor) as a function of filling factor $\langle n \rangle$, computed for an 8×8 instead of a 4×4 lattice as in the previous figure. The bottom panel is a blowup of the low-density region of the top panel. The solid line is for the $U=0$ case. For the two curves right above the $U=0$ case, the full vertex Γ is approximated by the T matrix with no self-energy effects, as in the bulk of the present paper. [This can be seen as keeping only the first term of the series for Γ in Eq. (C3), namely, $\Gamma^{(1)}$, and approximating $\Gamma^{(1)}$ by the T matrix.] The dash-dotted line shows the result when the full frequency dependence of the T matrix is taken into account, while in the calculation represented by the long-dashed line, the T matrix is approximated by its zero-frequency value. The two curves farther from the $U=0$ case and closest to the Monte Carlo results are obtained when the full integral equation (Ref. 32) for the vertex Γ in Eq. (C3) is solved (MCL approach), again replacing $\Gamma^{(1)}$ by the T matrix. The dotted line shows the result when the full frequency dependence of the T matrix is taken into account, while in the calculation represented by the dash-double-dotted line, the T matrix is approximated by its zero-frequency value.

$$f \approx \Gamma^{(1)}. \tag{C7}$$

Taking the above T-matrix approximation for $\Gamma^{(1)}$, this means that $f^{\uparrow\uparrow}=0$ and that the Landau parameter $f^a_{\mathbf{pp}'}$ necessary to compute, for example, the uniform magnetic susceptibility, can be obtained from

$$2f^a_{\mathbf{pp}'} = -f^{\uparrow\downarrow}_{\mathbf{pp}'} = -\Gamma^{(1)} = -\frac{U}{1+\chi_{pp}(\mathbf{p}+\mathbf{p}',\omega)U}. \tag{C8}$$

The momentum indices $\mathbf{p}$ and $\mathbf{p}'$ refer, respectively, to the momentum part of the indices 1 and 2 in the integral equation (C3). The momentum part of the index 5 is strictly zero, while there is left a small nonzero-frequency part denoted ω which must ultimately be taken to zero. The uniform magnetic susceptibility is then given by

$$\chi_s = \frac{\chi_0}{1+f^a_0\chi_0}, \tag{C9}$$

where $\chi_0 \equiv \chi_0(\mathbf{q}=0,\omega=0)$ reduces to the two-spin density of states at the Fermi surface at low temperature. Since f^a_0 represents the coefficient of the zeroth Legendre polynomial in the expansion of $f^a_{\mathbf{pp}'}$ over the Fermi surface, the last result (C9) is exactly the one which would be obtained from the GRPA with a renormalized value $U_{rn}=-2f^a_0$ computed from the T-matrix expression (C8) as follows: Take $\mathbf{p}$ and $\mathbf{p}'$ both on the Fermi surface, and average over the angle between both vectors. The explicit expression (C8) for the Landau parameter has a finite limit as frequency or temperature vanish, despite an apparent $1/\ln(\omega)$ singularity in the two-dimensional T matrix when one starts from high frequency.[9,34] In practice, it is convenient to work at small finite temperature and zero Matsubara frequency, as described below.

In Ref. 10, the average was taken over the whole Brillouin zone instead of over the Fermi surface. This is because in finite systems, there are very few points on the Fermi surface. As shown by Groleau[35] (Fig. 13), it turns out that both approaches give comparable results. To average over the Fermi surface in Fig. 13, Groleau used a lattice sufficiently large that at inverse temperatures $\beta=10/t$, the result did not depend on size anymore. Wave vectors were considered on the Fermi surface if their energy was within $1/\beta$ of the chemical potential, mimicking the finite frequency appearing in the expression (C8) for the Landau parameters. Also, both $\mathbf{p}$ and $\mathbf{p}'$ were varied around the Fermi surface to take into account the case of nonspherical Fermi surfaces. Two more checks were made:[35] (a) It does not matter whether one averages over wave vectors within $3/\beta$ or within $1/\beta$ of the chemical potential, indicating that the finite but low-frequency limit has been attained. (b) Averaging directly χ_{pp} in the denominator of (C8) gives results very similar to averaging the whole expression.[36] The latter averaging procedure has the advantage that one obtains a general expression relating the bare value of U to the renormalized value U_{rn} in the GRPA approach. Here is one final important note on this calculation of the Landau parameter corresponding to U_{rn}: In Ref. 10, the value of U_{rn} was also obtained by fitting the overall Monte Carlo data for the magnetic structure factor to a GRPA form.

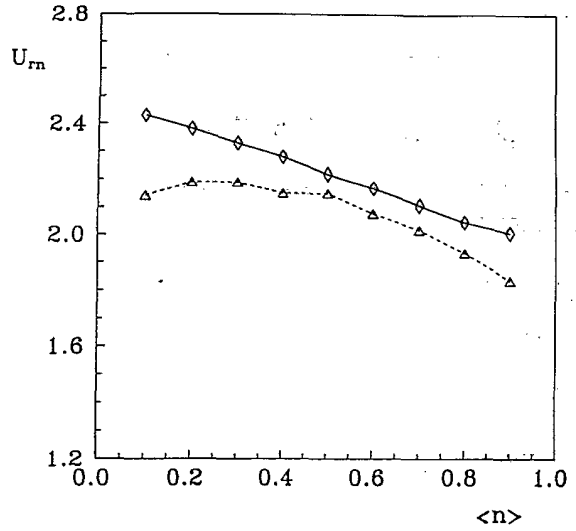

FIG. 13. Renormalized value of $U_{rn}=-2f_0^a$ as a function of the filling factor, obtained in two ways: by averaging expression (C8) over the Brillouin zone for an 8×8 system at $\beta=5$ as in Ref. 10 (solid line), and by averaging in an energy shell of thickness $1/\beta$ around the Fermi surface for a 40×40 system at $\beta=10$, as in Ref. 35 (dotted line). The latter approach corresponds to the Fermi-liquid prescription. The figure was taken from Ref. 35 with permission.

The value of U_{rn} obtained in this manner compares very closely to the value of U_{rn} found by the Fermi-liquid prescription used by Groleau. For example, for a bare value of U equal to $4t$, the value of U_{rn} obtained by fitting the Monte Carlo data is $2.2t$ at low density, in almost exact agreement with the Fermi-liquid prescription (dotted line in Fig. 13). The Brillouin-zone average gives instead $U_{rn}\approx2.5$. We should also point out that an alternate calculation of the Landau f function in two dimensions in the T-matrix approximation has appeared recently. It is shown explicitly in Ref. 34 that the appearance of a hole antibound state[24] in the T matrix does not invalidate Fermi-liquid theory.

The GRPA approach is probably valid only for weakly correlated Fermi liquids ($a\approx1$) contrary to Fermi-liquid theory, which is more general. On the other hand, when the GRPA approach is valid, it extends Landau Fermi-liquid theory in that it allows one to compute the magnetic structure factor for all wave vectors, not only $\mathbf{q}=\mathbf{0}$. A sufficient condition for the GRPA approach to be valid at arbitrary $\mathbf{q}$ when $a\approx1$ is that $\Gamma^{(1)}(1,2'+5;5)$ in the vertex Eq. (C3) depend very weakly on its momentum labels when 1 and $2'+5$ are both close to the Fermi surface. Continuing to approximate $\Gamma^{(1)}$ by the T matrix we see that it depends only on $1+2'+5$, not on 5 separately. Furthermore, the dependence on the precise value of $1+2'+5$ is not very large (predominant s-wave scattering) as follows from the near equality of the result obtained by either[36] averaging the full expression (C8) or just the denominator of the same expression.

This "GRPA with renormalized value of U" approach seems to be valid for a wider range of parameters (in particular, closer to half-filling) than is justified by the above arguments based on the MCL approach.[10,12] This suggests that, like Fermi-liquid theory, the structure of the theory at finite q remains the same with strong interactions as that with weak interactions, provided that renormalized (but hard to calculate) parameters are used.

[1]G. Baym and L. P. Kadanoff, Phys. Rev. **124**, 287 (1961); G. Baym, *ibid.* **127**, 1391 (1962).

[2]N. E. Bickers, Ann. Phys. (N.Y.) **193**, 206 (1989).

[3]J. W. Serene and D. W. Hess, Phys. Rev. B **44**, 3391 (1991).

[4]C. De Dominicis and P. C. Martin, J. Math. Phys. **5**, 14 (1964); **5**, 31 (1964).

[5]N. E. Bickers, in *Proceedings of the Adriatico Research Conference on Strongly Correlated Electron Systems,* edited by Yu Lu (World Scientific, Singapore, 1991).

[6]P. C. E. Stamp, J. Phys. F **15**, 1829 (1985). This paper also contains a detailed review of spin-fluctuation theories. R. A. Smith, in *Condensed Matter Theories, Volume 5,* edited by V. C. Aguilera-Navarro (Plenum, New York, 1990).

[7]N. E. Bickers and S. R. White, Phys. Rev. B **43**, 8044 (1991).

[8]P. W. Anderson, Phys. Rev. Lett. **64**, 1839 (1990); P. C. E. Stamp, *ibid.* **68**, 2180 (1992); **68**, 3938(E) (1992).

[9]J. R. Engelbrecht and M. Randeria, Phys. Rev. Lett. **65**, 1032 (1990); Phys. Rev. B **45**, 12 419 (1992).

[10]Liang Chen, C. Bourbonnais, T. Li, and A.-M. S. Tremblay, Phys. Rev. Lett. **66**, 369 (1991).

[11]N. Bulut, in *Proceedings of the NATO Advanced Study Institute on Dynamics of Magnetic Fluctuations in High Temperature Superconductors,* edited by G. Reiter, P. Horsch, and G. Psaltakia (Plenum, New York, 1991).

[12]N. Bulut, D. J. Scalapino, and S. R. White, Phys. Rev. B **47**, 2742 (1993); D. J. Scalapino (unpublished).

[13]D. Coffey and K. S. Bedell, Phys. Rev. Lett. **71**, 1043 (1993).

[14]C. Bourbonnais, H. Nélisse, A. Reid, and A.-M. S. Tremblay, Phys. Rev. B **40**, 2297 (1989); S. Sorella, A. Parolla, M. Parrinello, and E. Tosatti, Europhys. Lett. **12**, 721 (1990).

[15]V. M. Galitskii, Zh. Eksp. Teor. Fiz. **34**, 151 (1958) [Sov. Phys. JETP **7**, 104 (1958)].

[16]K. A. Brueckner and C. A. Levinson, Phys. Rev. **97**, 1344 (1955); K. A. Brueckner and J. L. Gammel, *ibid.* **109**, 1023 (1958).

[17]J. Kanamori, Prog. Theory. Phys. **30**, 275 (1963).

[18]James F. Annett, Adv. Phys. **39**, 83 (1990). We use the notation for the tetragonal group, even though we are working in two dimensions.

[19]For a review, see, E. Y. Loh and J. E. Gubernatis, in *Electron Phase Transitions,* edited by W. Hauke and Y. V. Kopaev (Elsevier, Amsterdam, 1992), pp. 177–235; we use the low-temperature stabilized algorithm of S. R. White, D. J. Scalapino, R. L. Sugar, E. Y. Loh, J. E. Gubernatis, and R. T. Scalettar, Phys. Rev. B **40**, 506 (1989).

[20]P. Bénard, Liang Chen, and A.-M. S. Tremblay, Phys. Rev. B **47**, 15 217 (1993).

[21]Liang Chen and A.-M. S. Tremblay (unpublished).

[22]A. Moreo and D. J. Scalapino, Phys. Rev. B **43**, 8211 (1991); S. R. White, D. J. Scalapino, R. L. Sugar, N. E. Bickers, and R. T. Scalettar, *ibid.* **39**, 839 (1989).

[23]R. T. Scalettar, R. R. P. Singh, and S. Zhang, Phys. Rev.

Lett. **67**, 370 (1991); N. E. Bickers, Phys. Rev. B **45**, 7418 (1992); E. Dagotto, A. Kampf, and J. R. Schrieffer, Phys. Rev. Lett. **67**, 2918 (1991).

[24]This pole is interpreted in Ref. 9 as an excitation consisting of bound hole pairs. In the hole picture, it is a hole antibound state which mirrors the electron antibound state on the other side of the band, in accordance with the particle-hole symmetry of the nearest-neighbor Hubbard Hamiltonian; M. Randeria (private communication).

[25]H. Fukuyama, Y. Hasegawa, and O. Narikiyo, J. Phys. Soc. Jpn. **60**, 2013 (1991).

[26]A. Moreo, Phys. Rev. B **45**, 5059 (1992).

[27]Shoucheng Zhang, Phys. Rev. B **42**, 1012 (1990).

[28]S. Babu and G. E. Brown, Ann. Phys. **78**, 1 (1973); K. F. Quader, K. S. Bedell, and G. E. Brown, Phys. Rev. B **36**, 156 (1987).

[29]L. D. Landau, Zh. Eksp. Teor. Fiz. **35**, 97 (1959) [Sov. Phys. JETP **8**, 70 (1959)].

[30]A. A. Abrikosov, L. P. Gorkov, and I. E. Dzyaloshinski, *Methods of Quantum Field Theory in Statistical Physics* (Prentice Hall, Englewood Cliffs, NJ 1963), Chap. 4; P. Nozières, *Interacting Fermi Systems* (Benjamin, New York, 1964).

[31]R. Shankar, Rev. Mod. Phys. (to be published).

[32]In practice, the integral equation can be solved numerically when it is written for a contraction of the full vertex, namely, for the appropriate three-point function.

[33]It is clear that, with system size, the number of oscillations increases at the same time as their amplitude decreases as can be seen by comparing Figs. 11 and 12 which are done, respectively, for a 4×4 and an 8×8 lattice. The susceptibilities vanish for certain fillings on the 4×4 lattice when a large gap exists at the Fermi surface due to finite level separation.

[34]J. R. Engelbrecht, M. Randeria, and L. Zhang, Phys. Rev. B **45**, 10 135 (1992). Note that $f^{\uparrow\uparrow}$ vanishes in our approach, contrary to the results of this paper.

[35]D. Groleau, M.Sc. thesis, Université de Sherbrooke, 1992 (unpublished), Appendix C.

[36]The (Cooper) logarithmic divergence in $\chi_{pp}(\mathbf{p}+\mathbf{p}',0)$ as $\mathbf{p}+\mathbf{p}'$ approaches zero is integrable, hence it does not cause problems when computing averages over the angle between $\mathbf{p}$ and $\mathbf{p}'$.